Solar Energy Materials & Solar Cells 92 (2008) 1586–1592

Contents lists available at ScienceDirect

Solar Energy Materials & Solar Cells

journal homepage: www.elsevier.com/locate/solmat

Fabrication and transport mechanisms of 2-(2,3-dihydro-1,5-dimethyl-3-oxo-2-phenyl-1*H*-pyrazol-4-ylimino)-2-(4-nitrophenyl)acetonitrile/p-silicon hybrid solar cell

H.M. Zeyada [a,*], M.M. El-Nahass [b], E.M. El-Menyawy [c]

[a] Physics Department, Faculty of Science at Damietta, 34517 New Damietta, Egypt
[b] Physics Department, Faculty of Education, Ain Shams University, Roxy, Cairo 11757, Egypt
[c] Physics Department, Solid State Electronics, National Research Center, Dokki, Cairo 12622, Egypt

ARTICLE INFO

Article history:
Received 15 November 2007
Received in revised form
26 March 2008
Accepted 12 July 2008
Available online 16 August 2008

Keywords:
Organic/Inorganic
Solar cells
Antipyrine derivative

ABSTRACT

2-(2,3-Dihydro-1,5-dimethyl-3-oxo-2-phenyl-1*H*-pyrazol-4-ylimino)-2-(4-nitrophenyl) acetonitrile (DOPNA) is an organic compound; it has been synthesized and examined as a photovoltaic material in thin-film form grown on single crystal of p-type silicon wafer substrate (p-Si). A polycrystalline structure has been formed in as-synthesized powder. Nano-crystallite grains are formed in the as-deposited film. The dark current–voltage (*I–V*) characteristics of Au/p-DOPNA/p-Si/Al heterojunction diode measured at different temperatures ranging from 298 to 423 K have been investigated. The operating conduction mechanisms, series and shunt resistances, rectification ratio, ideality factor and potential barrier height were determined. The capacitance–voltage (*C–V*) measurements of the device were performed in dark condition and analyzed to determine carrier concentration and built-in potential. Solar cell parameters were also evaluated and the power conversion efficiency was estimated as 5.74%.

1. Introduction

There is a significant jump of interest in solar cells made form organic compounds since the year of 2000 [1,2]. Fabrication methods and alternative materials have been investigated with the purpose of producing solar cells of high efficiency and low cost of production. One type of hybrid heterojunction solar cells consists of low-cost organic semiconductor combined with stable inorganic substrates. Recently, this type of planar heterojunction solar cells such as quaterthiophene/n-type GaAs or Si [3], hetrocycleamine organic layer containing N, S, P, Cl and J atoms/Si [4], 4-tricyanovinyl-*N*,*N*-diethylaniline/p-Si [5] and CuPc/n-GaAs [6] have been constructed and investigated.

Inorganic substrate effect on structure formation and efficiency of organic–inorganic solar cells were investigated [3]; the results showed that quaterthiophene deposited by thermal evaporation on GaAs substrates forms films consisting of grains of some hundred nanometers and large lamella defects; however, in the case of Si as substrate, almost defect-free highly ordered films with grain sizes of several micrometers up to a film thickness of 250 nm are formed. A maximum efficiency of 0.9% and 1.6% was obtained for quaterthiophene/n-Si and quaterthiophene/GaAs, respectively.

The effect of organic layer on Si solar cell performance was studied [4,5]. The Gorback et al. [4] design comprises of Si solar cell structure with patterned n^+p junction and heterocycleamine organic layer containing N, S, P, Cl and J atoms. The initial solar cell structure exhibited an efficiency of about 4–7% at AM0. The organic layer was grown from aquatic solution at room temperature and appropriate contact time between the solution and n^+p Si substrate. After the layer deposition, improvements in the solar cell performance were observed: short-circuit current, I_{sc}, doubled; open circuit voltage, V_{oc}, increased up to 50 mV, filling factor, FF, increased by 20% and the power conversion efficiency grew by 15%. El-Nahass et al. [5] constructed a hybrid solar cell from 4-tricyanovinyl-*N*,*N*-diethylaniline/p-Si, their results showed that the junction is of abrupt nature and it exhibits a power conversion efficiency of 3.1%. The effect of γ-ray irradiation (10 kGy absorbed dose) on the characteristics of the cell was also investigated; the fill factor (FF) and the power conversion efficiency of the cell decreased by 21% and 39% of the original value, respectively.

Photoelectrical and frequency response of p-CuPc/n-GaAs single crystal were investigated [6] in the temperature interval of 23–74 °C over the frequency range 0.01–100 kHz. The cell parameters such as rectification ratio (RR), threshold voltage,

* Corresponding author. Fax: +20572403868.
E-mail address: hamdyzeyada@yahoo.com (H.M. Zeyada).

0927-0248/$ - see front matter © 2008 Elsevier B.V. All rights reserved.
doi:10.1016/j.solmat.2008.07.006

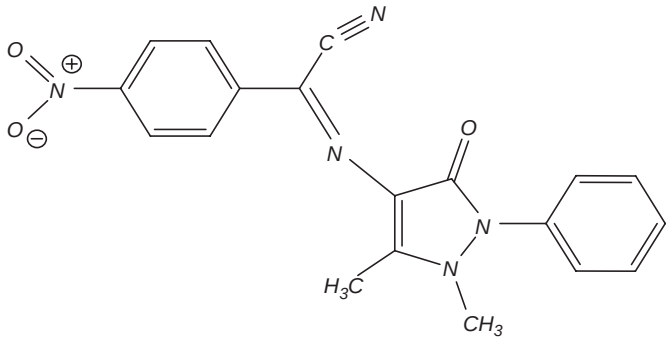

Fig. 1. Molecular structure of DOPNA compound.

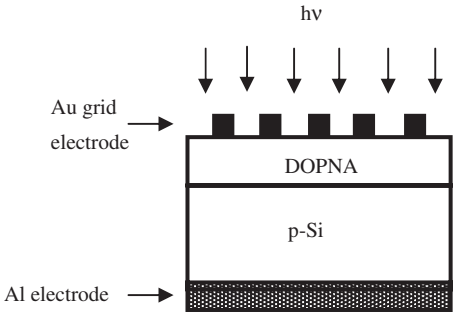

Fig. 2. Schematic diagram of the Au/p-DOPNA/p-Si/Al heterojunction diode.

nonlinearity coefficient, series and shunt resistance, diode ideality factor and power conversion efficiency are temperature dependent. The open circuit voltage decreases with an increase in frequency, whereas short-circuit AC current falls of with frequency but remains constant as a function of temperature.

In this work, 2-(2,3-dihydro-1,5-dimethyl-3-oxo-2-phenyl-1*H*-pyrazol-4-ylimino)-2-(4-nitrophenyl) acetonitrile compound (p-DOPNA) was synthesized from antipyrine derivative. The molecular structure of such a compound is shown in Fig. 1; a hybrid solar cell was designed as shown schematically in Fig. 2. The dark electrical characteristics of Au/p-DOPNA/p-Si/Al device have been studied with the purpose of determining the operating conduction mechanisms and parameters. The dynamic capacitance–voltage (*C–V*) method was also applied for determining carrier's concentration, built-in voltage and type of formed junction. The photovoltaic properties of Au/p-DOPNA/p-Si/Al heterojunction device were also determined.

2. Experimental procedure

2.1. Synthesis of the semiconductor compound

All the chemicals used in this study were obtained from Aldrich company and used as it was without any further purification. A mixture of 4-nitrobenzyl cyanide (1.62, 10 mmol) and 1,2-dihydro-2,3-dimethyl-4-nitroso-1-phenylpyrazol-5-one (2.17, 10 mmol) in ethanol (50 ml) containing a catalytic amount of piperidine (0.2 ml) was added. The reaction mixture was refluxed for 2 h and the deposited solid was collected by filtration and recrystallization from ethanol/benzene to give 2-(2,3-dihydro-1,5dimethyl-3-oxo-2-phenyl-1*H*-pyrazol-4-ylimino)-2-(4-nitrophenyl)acetonitrile as brown crystals; in yield 90%, melting point, m.p, 208–210 °C. IR (υ_{max}/(cm^{-1})): 1508.0 (conjugated nitro group); 1600.2 (aromatic ring); 1663.3 (imino group); 2196.6 (conjugated CN); 1744.1 (CO, antipyrinyl); 2853.0 (methyl group); 2924.7 (N-methyl group); ^{1}H NMR (DMSO-d_6)(δ, ppm): 3.34 (s, 3H, CH3); 3.38 (s, 3H, N-CH_3); 7.52 (m, 5H aromatic H); 8.25 (d.d, 4H aromatic H). Analysis calculated for $C_{19}H_{15}N_5O_3$: C, 63.15%; H, 4.18%; N, 19.38%. Found: C, 63.20%; H, 4.12%; N, 19.40%.

2.2. Device construction and measurements

Single crystal of (p-Si) wafer oriented at ⟨100⟩ with a thickness of 0.45 mm and carrier concentration of $10^{22}\,m^{-3}$ is obtained from Nippon mining company. The p-Si wafer was etched in a solution containing hydro-fluoric, nitric and acetic acids in the ratio of 1:6:1 to remove the native oxide. After etching, the p-Si wafer was immersed and washed with distilled water and finally with ethyl alcohol. The p-Si wafer was inserted in a vacuum coating unit and an ohmic contact of back side of Si wafer was made by coating it with a thick pure aluminum film. At the front side of the p-Si wafer substrate, a thin layer (86 nm) of p-DOPNA was deposited through a special mask followed by deposition of thin film of pure gold (60 nm) through another one. Then, Au/p-DOPNA/p-Si/Al device was constructed with a photo active area of 0.282 cm^2.

The films of p-DOPNA in this study were thermally deposited on the substrates by using a high-vacuum coating unit (model E306 A, Edwards Co.-England); the pressure inside the chamber was pumped down to 5×10^{-4} Pa before starting the evaporation process. A mechanical shutter was used to avoid any contamination on the substrate in the first stage of the evaporation process and to control the film thickness. DOPNA was sublimated under vacuum using quartz crucible that was subjected to induction heating by molybdenum heater. The rate of deposition and film thickness were controlled and adjusted during the evaporation by using a quartz crystal thickness monitor (model TM-350, Maxtek Inc.). The deposition rate was controlled at about 0.25 nm/s. The gold and aluminum electrodes were evaporated directly from boat-shaped molybdenum and basket-shaped tungsten filaments, respectively.

An X-ray diffractometer (Philips X″ pert, Pro.) with filtered CuKα radiation was used to investigate the structural properties of the DOPNA compound in powder and thin-film forms for the (2θ) diffraction angle range (4–60°). The applied voltage and tube current were 40 kV and 30 mA, respectively. JEOL JEM-1230 transmission electron microscope (TEM) was used to determine the crystallite shape and size of DOPNA thin films. The applied voltage was 80 kV.

For the current versus voltage (*I–V*) measurements at different temperatures, stabilized power supply and high impedance electrometer (Keithly 617) were used. The room temperature *C–V* measurements of the device were achieved at 1 MHz by using computerized *C–V* meter (model 4108, solid state measurements, Inc. Pittsburgh) in air and at dark conditions. The temperature of the sample was recorded during the electrical measurements by using NiCr–NiAl thermocouple with an accuracy of ±1 K. Photocurrent–voltage characteristics were carried out by using an ordinary tungsten filament lamp. The incident light falls normally on the device through the gold grid from the organic side. The intensity of the light was recorded with a calibrated digital light lux meter situated in the same position of the sample of interest and calculated as 80 W/m^2.

3. Results and discussion

3.1. Structural analyses

The X-ray diffraction (XRD) patterns of p-DOPNA in powder and as-deposited film (850 nm) conditions are depicted in

Figs. 3(a, b). DOPNA in as-synthesized condition shows a polycrystalline structure as shown in Fig. 3(a). Results showed also that the film deposited at room temperature is of nano-crystalline nature (Fig. 3(b)). A preferred orientation is also formed in as-deposited films. These results are confirmed by those obtained by TEM, and illustrated in Fig. 4; it shows nano-crystallites formed from nano-rods having a length and width of 116 and 32 nm, respectively.

3.2. DC dark conduction processes

The dark DC (I–V) characteristics of Au/p-DOPNA/p-Si/Al heterojunction solar cell measured at different temperatures ranging from 298 to 423 K at 25 K intervals and in the voltage range −2 to 2 V are depicted in Fig. 5. The results show typical diode behavior and at a certain applied voltage, the current increases with increasing temperature, indicating a negative temperature coefficient for the resistivity [7]. The low and weak voltage dependence of the reverse bias current as well as the strong voltage dependence of the forward bias current are characteristic properties of strong rectification performance for the junction diode interface; the RR has been estimated to be 1253 at ±1 V for room temperature. The value of the RR is relatively high although the DOPNA is a p-type semiconductor as observed from experiments in our laboratory; this is probably due to the difference in the work functions of p-DOPNA and p-Si as well as the type of conduction in this voltage range [8]. It was found that oxygen doping can improve the RR [8]. Other diode parameters such as series and shunt resistances (R_s and R_{sh}) were estimated at room temperature as 9.24 Ω and 219.78 kΩ, respectively.

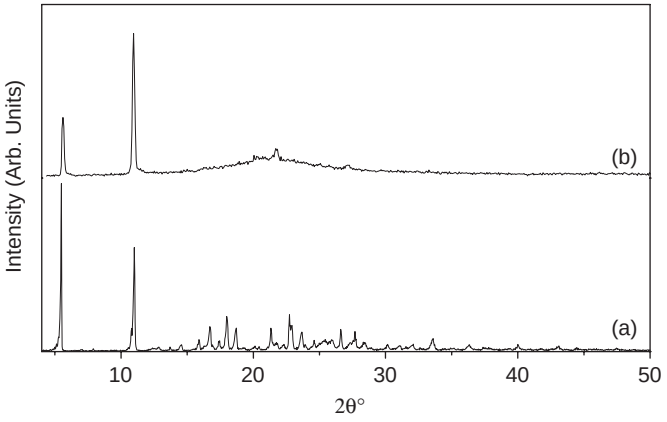

Fig. 3. XRD patterns of p-DOPNA compound: (a) as-synthesized powder and (b) as-deposited thin film with a thickness of 850 nm.

The semi-logarithmic plot characteristics of forward current versus voltage for Au/p-DOPNA/p-Si/Al device measured at room temperature are shown in Fig. 6. Results show that at relatively low forward bias ($V \leqslant 0.14$ V), Ln I–V relation is linear and the current of the device obeys the thermo-ionic emission of holes from p-DOPNA over the organic/inorganic (O/I) barrier in the device. The diode current expression for this conduction mechanism is given by [9,10]

$$I = I_s\left(\exp\left(\frac{eV}{nk_BT}\right) - 1\right) \quad (1)$$

where e is electronic charge, V the applied voltage across the device, k_B the Boltzmann's constant, T the absolute temperature and n the diode ideality factor. The value of n is estimated from the slope of the curve at room temperature in Fig. 6 as 1.13; this value is similar to that of p-type organic grown on p-Si [11]. The device was non-ideal in showing the value of $n > 1$; the n value is a result of recombination of electrons and holes in the depletion region and/or the increase of diffusion current due to an increase of the applied voltage [12].

Furthermore, the saturation current I_s in (1) is expressed as

$$I_s = AA^{**}T^2 \exp\left(\frac{e\varphi_b}{k_BT}\right) \quad (2)$$

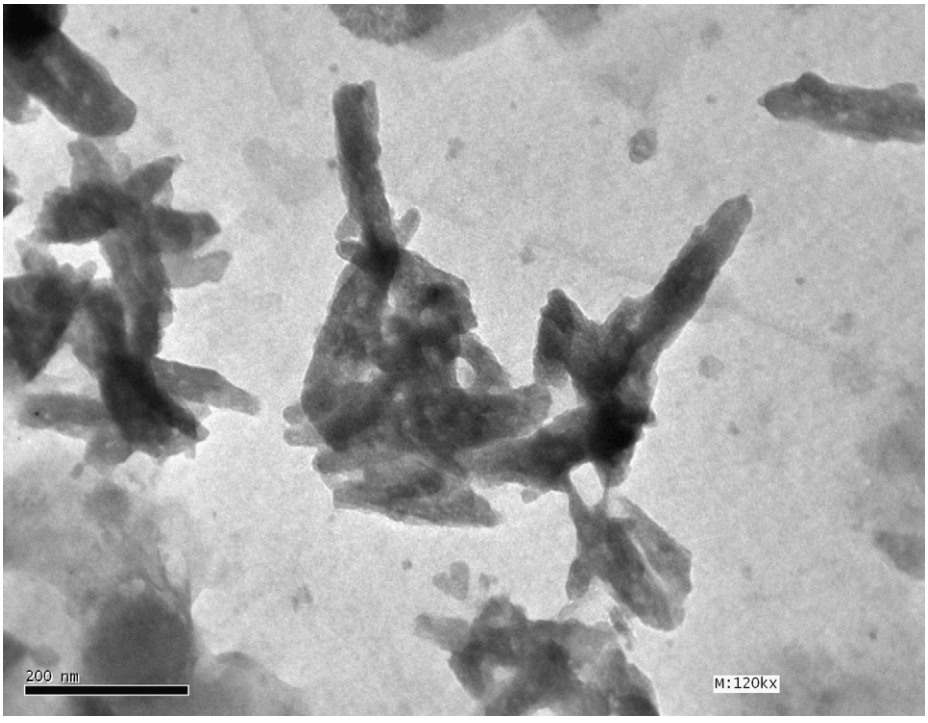

Fig. 4. Selected area TEM image of the as-deposited p-DOPNA thin film with magnification of 120k×.

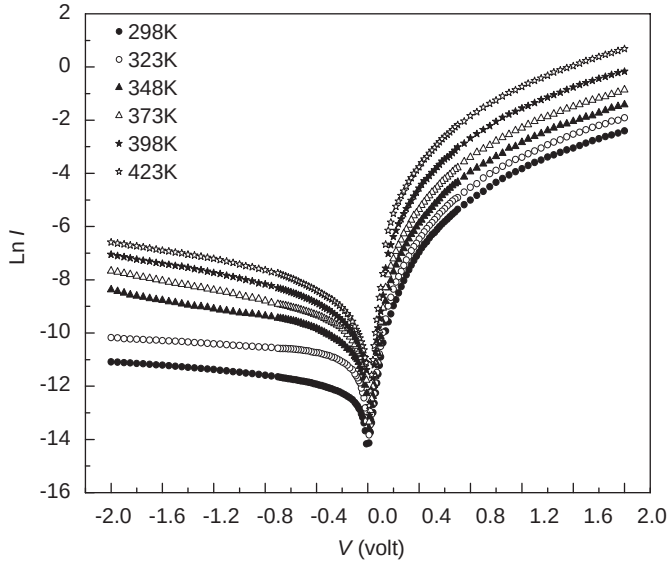

Fig. 5. Dependence of dark current on voltage for Au/p-DOPNA/p-Si/Al heterojunction measured at different temperatures ranging from 298 to 423 K at 25 K intervals.

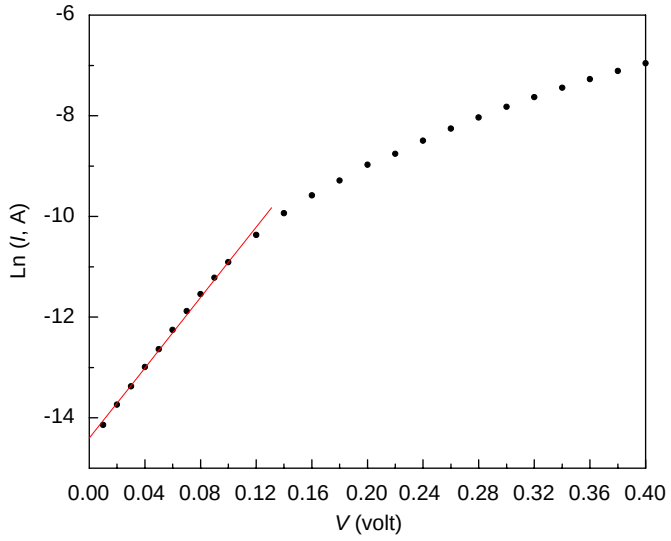

Fig. 6. Dependence of Ln(I) on forward bias voltage measured at room temperature.

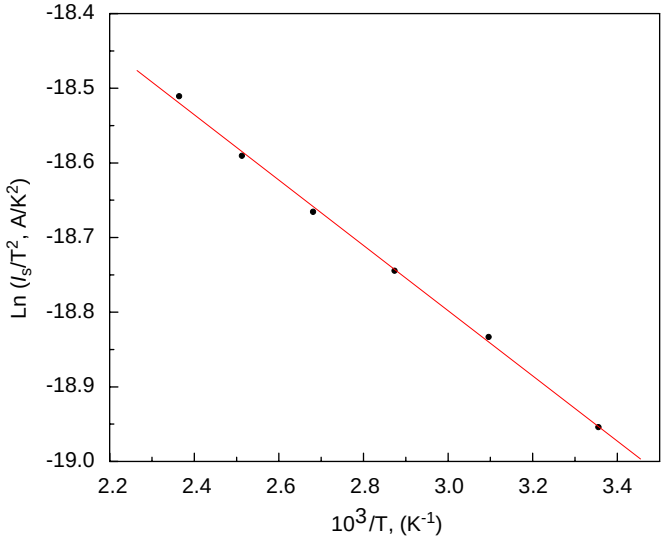

Fig. 7. Dependence of Ln(I_s/T^2) on reciprocal temperature for Au/p-DOPNA/p-Si/Al heterojunction diode at zero biasing.

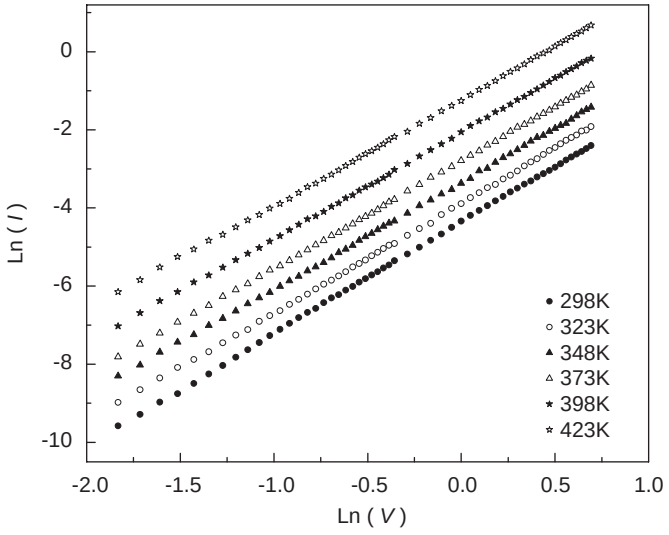

Fig. 8. Double-logarithmic plot of the forward bias (I–V) characteristic of Au/p-DOPNA/p-Si/Al heterojunction diode at different temperatures.

where A is the effective area of the device, A^{**} the Richardson's constant and φ_b the effective barrier height at the p-DOPNA/p-Si interface at zero bias. The saturation current was obtained at different temperatures from the intercept of the linear part in semi-logarithmic plot with the current axis at zero voltage (Fig. 5). The effective barrier height φ_b at zero bias was estimated from the slope in Fig. 7 together with Eq. (2) as 0.56 eV. It is well known in O/I devices that the value of n depends on electrode material [13], while the barrier height is roughly independent of metal used but it is indeed characteristic only of the O/I interface. The value of $n>1$ is an indicator of the presence of an insulator layer at the O/I interface [14]; probably an oxide layer is formed on the surface of Si substrate before the (p-DOPNA) organic thin-film deposition.

In the voltage range ($0.14<V\leqslant 2$), the double logarithmic plot of forward (I–V) characteristics at different temperatures is shown in Fig. 8. The results exhibit a super-linear relation with slope decreasing slightly from 2.86 to 2.7 with increasing temperature. This result indicates that the current follows the voltage dependence of the form $I \propto V^m$ with value of the exponent m greater than 2, which means that the current in the device is the space charge limited conduction dominated by exponential trap distribution (TSCLC). The current density for this particular case is described by [15]

$$J = e\mu N_v \left(\frac{\varepsilon}{eP_0 k_B T}\right)^l \frac{V^{l+1}}{d^{2l+1}} \tag{3}$$

where μ is the mobility of charge carrier, N_v the effective density of states at the valence band edge, ε the permittivity of the p-DOPNA thin film, P_o the trap concentration per unit energy range at the valence band edge and d the p-DOPNA film thickness. The term (l+1) represents the power law exponent, where $l = T_t/T$ and T_t is a temperature parameter characterizing the exponential trap distribution, which is given by

$$P(E) = P_0 \exp\left(\frac{-E}{k_B T_t}\right) \tag{4}$$

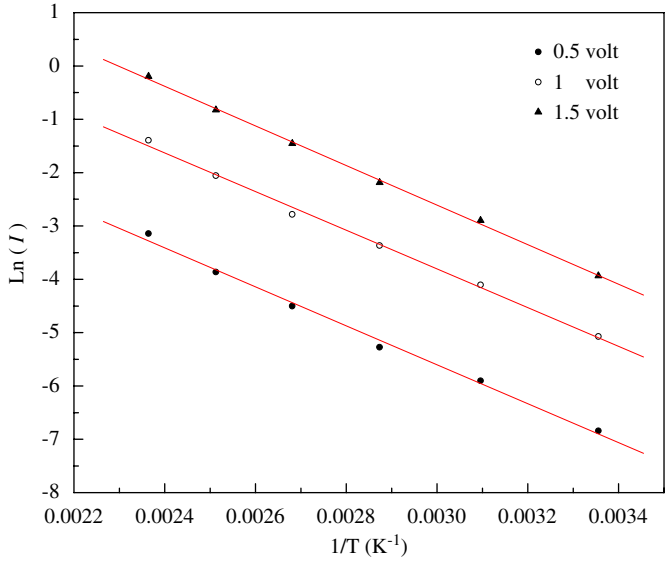

Fig. 9. Dependence of Ln(I) on reciprocal temperature for Au/p-DOPNA/p-Si/Al heterojunction diode at different bias potentials.

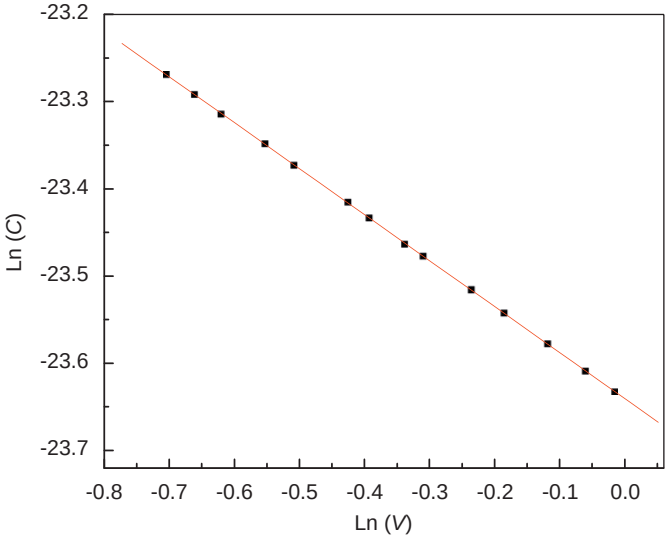

Fig. 10. Dependence of the junction capacitance on the reverse applied voltage for Au/p-DOPNA/p-Si/Al heterojunction diode measured at room temperature in dark condition.

$P(E)$ is the concentration of traps per unit energy range above the valence band edge. The total concentration of traps N_t is given by

$$N_t = P_0 k_B T_t \tag{5}$$

To estimate the values of parameters: N_t, T_t, l and P_o, the variation of Ln I versus $1/T$ at different applied voltages is shown in Fig. 9, the relation is linear and it has a slope, S, given by [15]

$$S = \frac{\Delta \mathrm{Ln}\, I}{\Delta(1/T)} = T_t \,\mathrm{Ln}(\varepsilon V / e d^2 N_t) \tag{6}$$

From optical properties work on p-DOPNA in our laboratory, a value of dielectric constant equal to 3.13 was evaluated. Substituting this value in Eq. (6), the total trap concentration, N_t, was estimated as 1.08×10^{25}, 2.5×10^{25} and $3.6\times10^{25}\,m^{-3}$ at 0.5, 1 and 1.5 applied voltages, respectively. Using an average value of $N_t \approx 2.39\times10^{25}\,m^{-3}$, the following values of trap parameters were derived at room temperature: $T_t \approx 554\,K$, $l = 1.86$ and $P_o = 3.13\times10^{45}\,J^{-1}\,m^{-3}$. The values of N_t and P_o seem to be reasonable in that they are of the same order as those by Anthopoulos and Shafia [16] deduced for freshly prepared samples and in low-applied-voltage regions ($N_t = 7.8\times10^{25}\,m^{-3}$ and $P_o = 6.4\times10^{45}\,J^{-1}\,m^{-3}$) for Au/Ni-phthalocyanine/Al homojunction diode.

3.3. Capacitance–voltage characteristics

The junction capacitance (C) of a diode as a function of the reverse bias voltage (V_r) is given by [17]

$$C = \frac{C_0}{(1+(V_r/V_a))^g} \tag{7}$$

where C_0 is the zero bias junction capacitance and g is a coefficient whose value depends on the nature of the junction. It takes the value of 1/2 and 1/3 for abrupt and linearly graded junctions, respectively. The parameter g is obtained by plotting the natural logarithm of the junction capacitance versus the natural logarithm of the reverse voltage (g is the slope of this curve) as shown in Fig. 10. The obtained value of g is equal to 0.53, indicating that the junction is of abrupt nature. Fig. 11 shows the (C^{-2}–V) characteristics at room temperature for Au/p-DOPNA/p-Si/Al device measured in dark condition. The capacitance was examined with the aid of usual Schottky relation which is modified by

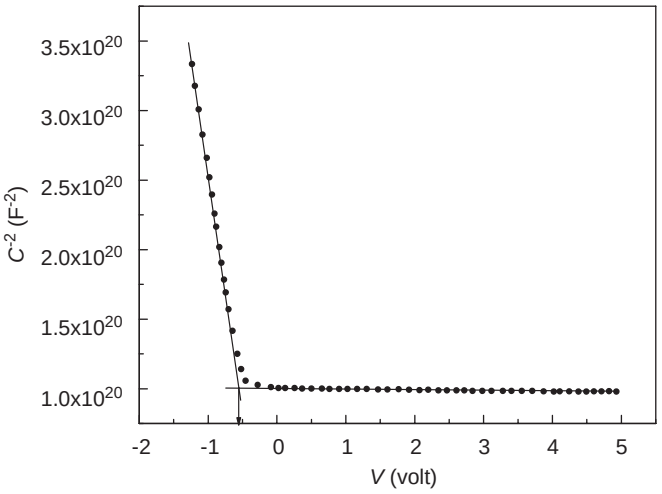

Fig. 11. Variation of C^{-2} with V for Au/p-DOPNA/p-Si/Al heterojunction diode measured at room temperature in dark condition.

Anderson for an abrupt junction [17]:

$$\frac{1}{C^2} = \frac{2(\varepsilon_d N_d + \varepsilon_a N_a)(V_b + V)}{e\varepsilon_d\varepsilon_a N_d N_a A^2} \tag{8}$$

where ε_d and ε_a are the permittivity of the donor and acceptor semiconductors, respectively, N_d and N_a are the carrier concentration of the ionized donor and acceptor atoms, V_b is the built-in potential, V the applied voltage and A the effective area of the device. From Eq. (8) it is clear that a plot of C^{-2} versus V should give a straight line; from the intercept with the voltage axis, the concentration of carriers is estimated as $1.61\times10^{27}\,m^{-3}$. According to Beth's model used in Ref. [18], the intercept of the C^{-2}–V plot with the horizontal asymptote, rather than the bias line leads to the value of the built-in potential V_b as given by Eq. (8). The asymptote is interpreted to represent the series geometrical capacitance. The value of built-in potential for the diode was estimated as 0.52 V; this value is comparable with the value of the barrier height (0.56 eV) predicted previously by thermo-ionic emission model.

3.4. Photovoltaic properties of the device

The (*I–V*) characteristic of Au/p-DOPNA/p-Si/Al heterojunction solar cell measured at room temperature in dark and under illumination conditions are shown in Fig. 12. It can be seen that at a certain voltage, the current value for the cell under illumination is higher than in the dark condition; this phenomenon is a result of the difference in the electron affinities of the two semiconductors [19]. On illumination, the light generates a photocurrent and its influence appears in the region of the fourth quadratic, which is plotted separately in Fig. 13. As can be seen, the values of the open circuit voltage (V_{oc}), the short-circuit current (I_{sc}), voltage at maximum power point (V_M) and the current at maximum power point (I_M) for the device were obtained as 0.29 V, 1.35 mA, 0.16 V and 0.8 mA, respectively. The FF is given by [7]

$$FF = V_M I_M / V_{oc} I_{sc} \quad (9)$$

The value of the FF was calculated as 0.33. The experimental power conversion efficiency of a solar cell is given by [7]

$$\eta = (FF V_{oc} I_{sc} / A P_{in}) \times 100\% \quad (10)$$

where P_{in} is the illumination intensity impinging on the cell and A the effective area. The efficiency of the cell was calculated as 5.74%.

The results shown in Table 1 indicate that the efficiency of a solar cell depends on the organic compound used for light harvesting. The DOPNA semiconductor organic compound satisfies the conditions imposed by Forrest et al. [13] on a particular organic molecule to form a high-quality rectifying contact barrier diode when deposited on an inorganic semiconductor substrate, i.e. the gold electrode makes an ohmic contact with p-DOPNA and at the same time it was deposited as masked network electrode to reduce optical filter effect. The deposited p-DOPNA film is grown as nano-rods; the electron transfer in nano-rods is much easier than the spherical particles [23]; this leads to the minimization of the electron losses at the grain boundaries and therefore better photo-conversion efficiency is obtained.

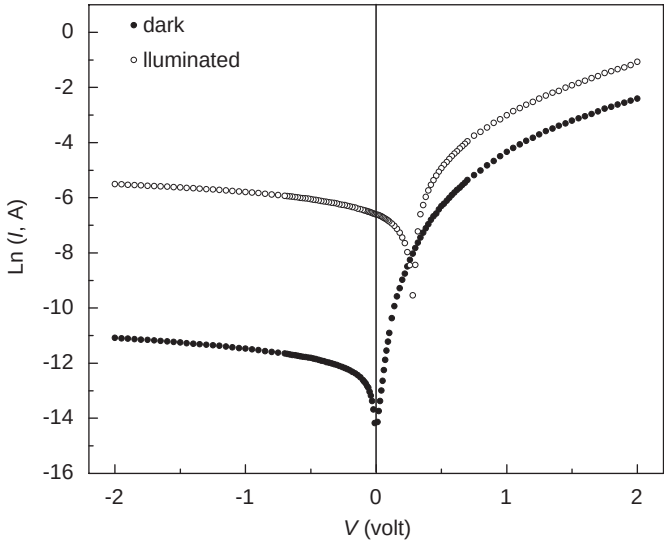

Fig. 12. (*I–V*) characteristic curves for Au/p-DOPNA/p-Si/Al heterojunction diode under dark and illumination conditions measured at room temperature.

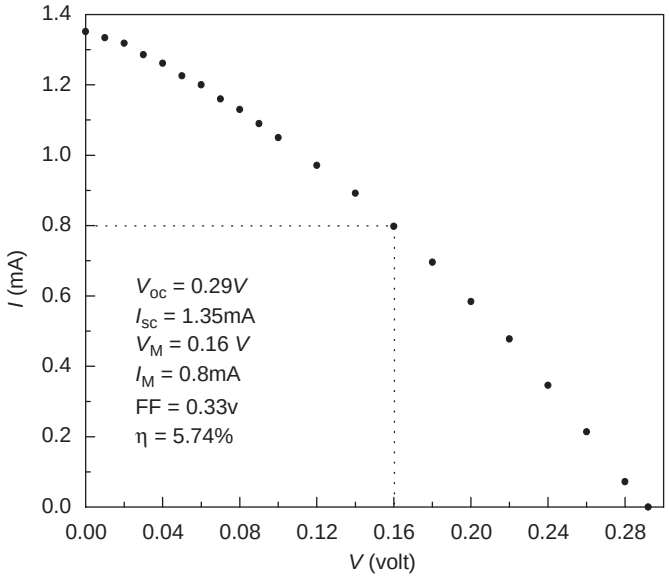

Fig. 13. (*I–V*) characteristic curve of maximum power region for Au/p-DOPNA/p-Si/Al heterojunction solar cell under illumination condition measured at room temperature.

4. Summary and conclusion

2-(2,3-Dihydro-1,5-dimethyl-3-oxo-2-phenyl-1*H*-pyrazol-4-ylimino)-2-(4-nitrophenyl)acetonitrile compound (DOPNA) has been synthesized. A polycrystalline structure has been formed in the as-synthesized powder. p-DOPNA films are grown by the conventional thermal evaporation technique as nano-crystallite rods. Hybrid Au/p-DOPNA/p-Si/Al heterojunction device was fabricated and showed low series resistance of 9.24 Ω, high shunt resistance of 219.78 kΩ and strong RR of 1253 at ±1 V and at room temperature. At relatively low voltages ($V \leqslant 0.14$), the current in the device follows the thermo-ionic emission model. The value of the barrier height at zero biasing was estimated as 0.56 eV. In the voltage range ($0.14 < V \leqslant 2$), the (*I–V*) characteristics showed that the space charge limited current dominated by exponential distribution of traps is the appropriate conduction mechanism; the value of the total trapping concentration and trap concentration per unit energy range at the valance band edge

Table 1
Photovoltaic parameters of some organic heterojunction solar cells

Solar cell construction	J_{sc} (mA/cm^2)	V_{oc} (volt)	Fill factor	Intensity of light (mA/cm^2)	Efficiency (%)	Ref.
Au/Mg-phthalocyanine/n-Si/Al	3.67	0.35	0.4	50	1.05	[20]
Au/Ni-phthalocyanine/p-Si/Al	9.2	0.32	0.28	6	1.11	[21]
Au/dicyclopropyl fulgide/ n-Si/Al	9.13	0.297	0.33	70	1.27	[22]
Au/tetraphenyl porphyrin/ n-Si/Al	2.76	0.25	0.37	20	2.45	[7]
Au/4-tricyanovinyl-N,N diethylaniline/p-Si/Al	9.15	0.7	0.39	80	3.1	[5]
Au/p-DOPNA/p-Si/Al	4.83	0.29	0.33	8	5.74	Present work

were estimated as $2.39 \times 10^{25}\,m^{-3}$ and $3.13 \times 10^{45}\,J^{-1}\,m^{-3}$, respectively. The C–V characteristics of the device were performed at room temperature in dark condition and the diode parameters such as built-in potential and carrier concentration were obtained as 0.52 V and $1.61 \times 10^{27}\,m^{-3}$, respectively. The ($I$–$V$) characteristic of the device under illumination with light of intensity $80\,W/m^2$ gives the values 0.29 V, 1.35 mA, 0.33 and 5.74% for the open circuit voltage (V_{oc}), short-circuit current (I_{sc}), fill factor (FF) and power conversion efficiency (η), respectively.

Acknowledgement

This work was financially supported by Mansoura University, Egypt.

References

[1] J. Nelson, Curr. Opin. Solid State Mater. Sci. 6 (2002) 87.
[2] J.M. Nunzi, C.R. Phys. 3 (2002) 523.
[3] J. Ackermann, C. Videlot, A. El Kassmi, Thin Solid Films 403 (2002) 157.
[4] T.Ya. Gorbach, P.S. Smertenko, S.V. Svechnikov a, M. Kuzma, Thin Solid Films 511 (2006) 494.
[5] M.M. El-Nahass, H.M. Zeyada, K.F. Abd-El-Rahman, A.A.A. Darwish, Sol. Energy Mater. Sol. Cells 91 (2007) 1120.
[6] Kh.S. Karimov, M.M. Ahmed, S.A. Moiz, M.I. Fedorov, Sol. Energy Mater. Sol. Cells 87 (2005) 61.
[7] M.M. El-Nahass, H.M. Zeyada, M.S. Aziz, M.M. Makhlouf, Thin Solid Films 492 (2005) 290.
[8] K.R. Rajesh, C.S. Menon, J. Non-Cryst. Solids 353 (2007) 398.
[9] M. Shimura, A. Toyoda, Jpn. J. Appl. Phys. 23 (1984) 1462.
[10] D.V. Morgan, Y. Aliyu, R.W. Bunce, Phys. Status Solidi A 133 (1992) 77.
[11] M. Çakar, A. Türüt, Y. Onganer, J. Solid State Chem. 168 (2002) 174.
[12] T.S. Shafai, T.D. Anthopoulos, Thin Solid Films 398 (2001) 361.
[13] S.R. Forrest, M.L. Kaplan, P.M. Schmidt, J. Appl. Phys. 56 (2) (1984) 543.
[14] M. Çakar, Y. Onganer, A. Türüt, Synth. Met. 126 (2002) 213.
[15] T.G. Abdel Malik, R.M. Abdel-Latif, Thin Solid Films 305 (1997) 336.
[16] T.D. Anthopoulos, T.S. Shafia, J. Phys. Chem. Solids 64 (2003) 1217.
[17] S.M. Sze, Physics of Semiconductor Devices, Wiley, New York, 1983, p. 97.
[18] T.D. Anthopoulos, T.S. Shafai, J. Phys. Chem. Solids 65 (2004) 1345.
[19] M.M. El-Nahass, A.M. Farid, A.A.M. Farag, H.A.M. Ali, Vacuum 81 (2006) 8.
[20] S. Riad, Thin Solid Films 370 (2000) 253.
[21] M.M. El-Nahass, K.F. Abd-El-Rahman, A.A.M. Farag, A.A.A. Darwish, Org. Electron. 6 (2005) 129.
[22] M.M. El-Nahass, H.M. Zeyada b, A.A. Hendi, Eur. Phys. J. Appl. Phys. 25 (2004) 85.
[23] N. Beermann, L. Vayssieres, S.E. Lindquist, A. Hagfeldtz, J. Electrochem. Soc. 147 (2000) 2456.